Measurement errors induced by axis tilt of biplates in dual-rotating compensator Mueller matrix ellipsometers

Honggang Gu [1], Chuanwei Zhang [1,2], Hao Jiang [1], Xiuguo Chen [1], Weiqi Li [1], and Shiyuan Liu [1,2,*]

[1] *State Key Laboratory of Digital Manufacturing Equipment and Technology, Huazhong University of Science and Technology, Wuhan 430074, China*

[2] *Wuhan Eoptics Technology Co., Ltd., Wuhan 430075, China*

ABSTRACT

Dual-rotating compensator Mueller matrix ellipsometer (DRC-MME) has been designed and applied as a powerful tool for the characterization of thin films and nanostructures. The compensators are indispensable optical components and their performances affect the precision and accuracy of DRC-MME significantly. Biplates made of birefringent crystals are commonly used compensators in the DRC-MME, and their optical axes invariably have tilt errors due to imperfect fabrication and improper installation in practice. The axis tilt error between the rotation axis and the light beam will lead to a continuous vibration in the retardance of the rotating biplate, which further results in significant measurement errors in the Mueller matrix. In this paper, we propose a simple but valid formula for the retardance calculation under arbitrary tilt angle and azimuth angle to analyze the axis tilt errors in biplates. We further study the relations between the measurement errors in the Mueller matrix and the biplate axis tilt through simulations and experiments. We find that the axis tilt errors mainly affect the cross-talk from linear polarization to circular polarization and vice versa. In addition, the measurement errors in Mueller matrix increase acceleratively with the axis tilt errors in biplates, and the optimal retardance for reducing these errors is about 80°. This work can be expected to provide some guidences for the selection, installation and commissioning of the biplate compensator in DRC-MME design.

Keywords: dual-rotating compensator Mueller matrix ellipsometer; biplate; axis tilt; measurement errors; accuracy.

1. INTRODUCTION

The dual-rotating compensator Mueller matrix ellipsometer (DRC-MME) has been designed and applied as a powerful tool for nanostructure metrology in high-volume nanomanufacturing [1-4]. The compensators also called optical retarders are indispensable optical components and their performances affect the precision and accuracy of the DRC-MME significantly. Biplates made of birefringent crystals such as magnesium fluoride (MgF_2) and quartz are the most commonly used compensators in the DRC-MME [5-7]. A single-waveplate is a slice of birefringent crystal usually cut with the optic axis lying on the plane of the plate. And a biplate is composed of two single-waveplates made of the same material whose optic axes are strictly aligned perpendicular to each other [8]. The optical properties of the biplate, such as the retardance and the axis azimuth, are sensitive to the optic axis orientation and thickness of the crsystal, the wavelength and view angle of the incident light, and the temperature and humidity of the surroundings [9]. In practice, the biplate invariably has variety of errors due to imperfect manufacturing and improper installation. These errors indubitably have great influences on the final measurement results of the DRC-MME. Therefore, studying the relations between the measurement results and these errors is of great importance to improve the measurement precision and accuracy of the DRC-MME.

Many researchers have devoted their efforts to explore the influence mechanism of these errors arising from the manufacturing and installing processes of biplates. P. D. Hale and G. W. Day studied the effects of changes in incident angle, wavelength and temperature on the retardance of birefringent waveplates [9]. E. A. West *et al* and B. Boulbry *et al* studied polarization errors associated with birefringent biplates, and these errors include thickness errors, optic axes misalignment errors, field-of-view errors and optic axis tilt errors [10-11]. K. Ebert *et al* and P. Marsik *et al* showed that the rotating-compensator ellipsometers would suffer from various artifacts due to the interference effect and misalignment

errors of bipalte compensators [12-13]. H. Dong *et al* and H. Dai *et al* presented measurement errors induced by retardance deviation and misalignment errors of the rotating waveplates in Stokes polarimeters [14-16]. In our previous work, the misalignment errors in rotating waveplates of the DRC-MME are studied and calibrated [17]. Most of the published literatures concentrate on the static errors of the biplates, such as retardance errors, misalignment errors, and field-of-view errors, which usually can be corrected or compensated through a system calibration procedure. However, if the rotation axis of the biplate is not parallel to the light beam due to improper installation and commissioning procedure, dynamic artifacts, such as beam wander and retardance vibration [18], will be introduced, since the biplates are continuously rotating in the DRC-MME. These dynamic errors are more complicate and usually hardly to be calibrated.

In this paper, we attempt to study and reduce the measurement errors induced by the axis tilt errors of biplates to improve the measurement accuracy of the DRC-MME. We propose a simple but valid formula to calculate the retardance of the rotating biplate compensator under arbitrary tilt angle and azimuthal angle based on the theory of wave propagation. Using the proposed formula, we analyze different kinds of axis tilt errors in the rotating biplate and discuss their effects on the measurement of the DRC-MME. We further study the relations between the measurement errors of the DRC-MME and the biplate axis tilt errors through simulations and experiments. A home-made DRC-MME prototype using MgF_2 biplates as the rotating compensators has been set up to perform the experiments. Simulated and experimental results on the measurement of the air Mueller matrix under different axis tilt errors in the biplate compensators are presented and discussed. This work can be expected to guide the selection and installation of the biplate compensators and the commissioning of the optical path of the DRC-MME to minimize or eliminate the measurement errors induced by the axis tilt errors of biplates.

2. AXIS TILT ERRORS IN BIPLATE

2.1 Retardance calculation of biplate

Biplates made of birefringent crystals are the most commonly used compensators in ellipsometry. The phase retardance of a biplate introduced by the birefringence and the optical path length in the crystal is given by

$$\delta = \frac{2\pi}{\lambda}\Delta n \cdot d,$$ (1)

where $\Delta n = n_e - n_o$ is the birefringence of the crystal, n_e and n_o are the extraordinary and the ordinary refractive indices, $d = d_1 - d_2$ is the effective thickness of the biplate, d_1 and d_2 are the thicknesses of the first and the second component plates of the biplate, and λ is the vacuum wavelength.
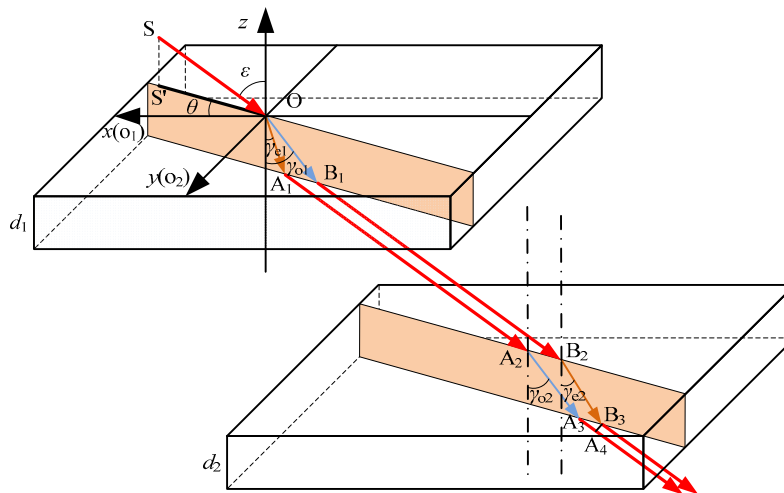
Figure 1. Schematic of the wave propagation in a biplate.

A bipalte is usually designed and used for normal incidence, but its retardance is sensitive to the incident angle of the light since both the optical path length and the extraordinary refractive index vary with the direction of light propagation. Strict calculation of the retardance for arbitrary incident angle can be achieved by using the ray-tracing formulas or

Maxwell's equations and boundary conditions [19-21]. However, these methods can be very complex. Here, we propose a simple formula to calculate the retardance of the biplate based the theory of wave propagation.

Figure 1 schematically shows the wave propagation in the biplate in a cartesian coordinate system assuming that the optic axes of the first plates and the second plates lie parallel to x-axis and y-axis, respectively. The light **SO** enters the biplate with an incident angle ε and an azimuth angle θ respect to x-axis, and **S'O** is the projection of **SO** on x-y plane. **OA$_1$** (**OB$_1$**) and **B$_2$B$_3$** (**A$_2$A$_3$**) are the wave normals for e-ray (o-ray) in the first and the second plates, and γ_{e1} (γ_{o1}) and γ_{e2} (γ_{o2}) are their refraction angles, respectively. According to snell's Law, we can obtain

$$\sin \varepsilon = n_{e1} \sin \gamma_{o1} = n_o \sin \gamma_{o1} = n_{e2} \sin \gamma_{e2} = n_o \sin \gamma_{o2}, \tag{2}$$

where n_{e1} and n_{e2} are the effective refractive indices of the extraordinary rays in the first and the second plates with respect to incident angle ε and azimuth angle θ of the incident light, and can be calculated as [22-23]

$$n_{e1} = n_e \left[1 + \left(\frac{1}{n_e^2} - \frac{1}{n_o^2} \right) \sin^2 \varepsilon \cos^2 \theta \right], \tag{3a}$$

$$n_{e2} = n_e \left[1 + \left(\frac{1}{n_e^2} - \frac{1}{n_o^2} \right) \sin^2 \varepsilon \sin^2 \theta \right]. \tag{3b}$$

According to the theory of wave propagation, the phase retardance between the two rays exiting out from the biplate is given by

$$\delta = \frac{2\pi}{\lambda} \left(|OA_1| n_{e1} + |A_1 A_2| + |A_2 A_3| n_o + |A_3 A_4| - |OB_1| n_o - |B_1 B_2| - |B_2 B_3| n_{e2} \right)$$

$$= \frac{2\pi}{\lambda} \left[d_1 \left(\frac{n_{e1}}{\cos \gamma_{e1}} - \frac{n_o}{\cos \gamma_{o1}} \right) - d_2 \left(\frac{n_{e2}}{\cos \gamma_{e2}} - \frac{n_o}{\cos \gamma_{o2}} \right) + |A_3 A_4| \right], \tag{4}$$

where $|A_3 A_4|$ is the optical path difference in the air, and can be calculated using the geometric relationships

$$|A_3 A_4| = |A_3 B_3| \sin \varepsilon = \left(|OB_1| \sin \gamma_{o1} - |OA_1| \sin \gamma_{e1} + |B_2 B_3| \sin \gamma_{e2} - |A_2 A_3| \sin \gamma_{o2} \right) \sin \varepsilon$$

$$= \left[d_1 (\tan \gamma_{o1} - \tan \gamma_{e1}) - d_2 (\tan \gamma_{o2} - \tan \gamma_{e2}) \right] \sin \varepsilon. \tag{5}$$

Substituting Eq. (2)-(3) and Eq. (5) into Eq. (4), we obtain

$$\delta(\varepsilon, \theta) = \frac{2\pi}{\lambda} d_1 \left(\sqrt{ n_e^2 - \frac{n_e^2 \cos^2 \theta + n_o^2 \sin^2 \theta}{n_o^2} \sin^2 \varepsilon } - \sqrt{ n_o^2 - \sin^2 \varepsilon } \right)$$

$$- \frac{2\pi}{\lambda} d_2 \left(\sqrt{ n_e^2 - \frac{n_e^2 \sin^2 \theta + n_o^2 \cos^2 \theta}{n_o^2} \sin^2 \varepsilon } - \sqrt{ n_o^2 - \sin^2 \varepsilon } \right). \tag{6}$$

Equation (6) gives a general formula for retardance calculation of a biplate under arbitrary incident angle and arbitrary azimuthal angle. To verify the validity of the formula, we have performed experiments on an MgF$_2$ biplate (a commercial zero-order half wavepalte at 193nm from B-halle) whose total thickness is about 1.6mm. As shown in Fig. 2, the high agreement between the experimental results and calculated results demonstrates the correctness of the formula as well as the fact that the retardance deviates with the azimuthal angle and the incident angle when the light is oblique incident.
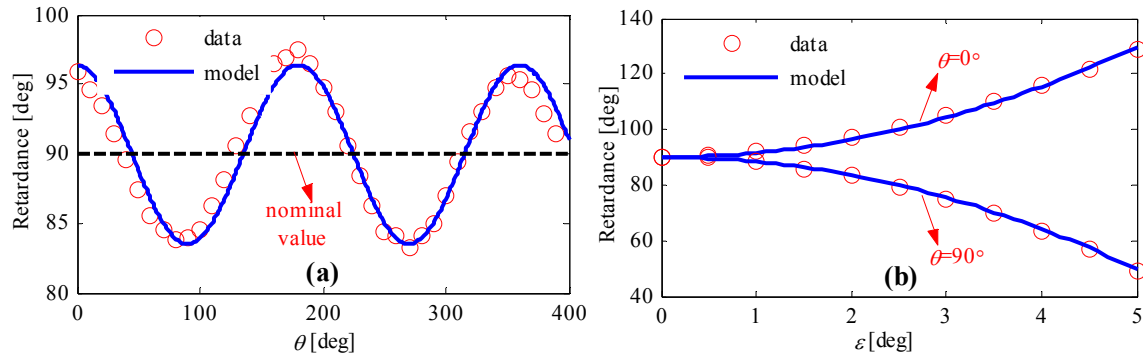
Fig. 2. Experimental results (red circle) and calculated results (blue solid line) of the vibrations in the retardance of the MgF$_2$ biplate. The experimental wavelength is 347nm, at which the nominal retardance is about 90°. (a) Vibration versus the rotation azimuth θ under a tilt error of 2°; (b) vibrations versus the tilt error ε at azimuths of 0° and 90°.

2.2 Axis tilt errors in biplate

During manufacturing and installation, the biplate invariably has variety of axis tilt errors which may further cause the light entering the plate at oblique incidence. In a rotating-compensator system, there are usually three possible kinds of axis tilt errors in the biplate as shown in Fig. 3. (1) The optic axis of the waveplate (F) is tilted off the plate plane due to imperfect fabrication, such as improper cut of the crystal. (2) The normal direction of the plate plane (N) is tilted off the rotation aixs (R) due to improper installation of the biplate. (3) The rotation axis is tilted off the beam (K) due to improper installation or improper commissioning of the optical path.
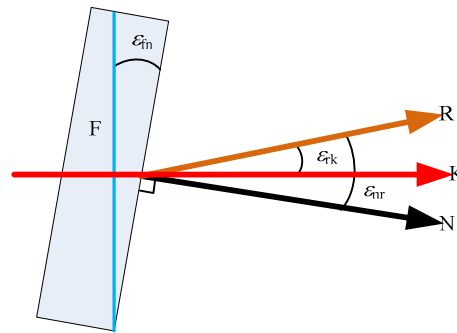
Fig. 3. Schematic of three possible kinds of axis tilt errors in the biplate. F, N, R and K refer to the optic axis of the biplate, the normal axis of the plate plane, the rotation axis and the beam, and ε_{fn}, ε_{nr} and ε_{rk} are the angle between F and N, the angle between N and R, and the angle between R and K.

Obviously, the former two kinds of axis tilt errors cause the light entering the biplate at a constant incident angle, i. e., the angle between F and N and the angle between F and R will not change during the rotation. According to Subsection 2.1, they only introduce a stationary bias in retardance from its nominal value which usually can be calibrated and corrected in an instrument [24]. In addition, they are usually very small that can be ignored. However, the last kind of axis tilt error causes a varied incidence (i.e. the angle between F and K) when the biplate continuously rotates with the motor that further results in a vibration in the retardance. Moreover, this kind of axis error is usually relatively large and is not negligible. Therefore we focus on the tilt error between the rotation axis and the beam in this paper, i.e., $\varepsilon_{fn} = \varepsilon_{nr} = 0$.

3. MEASUREMENT ERRORS INDUCED BY AXIS TITL IN DRC-MME

3.1 Basic principles and instrumentation of DRC-MME

As schematically shown in Fig. 4, the basic system layout of the DRC-MME in order of light propagation is PC$_{r1}(\omega_1)$SC$_{r2}(\omega_2)$A, where P and A stand for the polarizer and analyzer, C$_{r1}$ and C$_{r2}$ refer to the 1st and 2nd rotating compensators, and S stands for the sample. The fast axis angles C_1 and C_2 of the 1st and 2nd compensators rotate synchronously at $\omega_1 = 5\omega$ and $\omega_2 = 3\omega$, where ω is the fundamental mechanical frequency. The Stokes vector $\mathbf{S}_{out}$ of the exiting light beam can be expressed as the following Mueller matrix product [1, 3, 25]

$$\mathbf{S}_{\mathrm{out}} = \left[\mathbf{M}_A \mathbf{R}(A)\right]\left[\mathbf{R}(-C_2)\mathbf{M}_{C2}(\delta_2)\mathbf{R}(C_2)\right]\mathbf{M}\left[\mathbf{R}(-C_1)\mathbf{M}_{C1}(\delta_1)\mathbf{R}(C_1)\right]\left[\mathbf{R}(-P)\mathbf{M}_P\right]\mathbf{S}_{\mathrm{in}}, \qquad (7)$$

where $\mathbf{M}_i$ (i = P, A, C1, C2) is the Mueller matrix associated with each optical element. $\mathbf{R}(\alpha)$ is the Mueller rotation transformation matrix for rotation by the angle α [α = P, A, C_1, and C_2] that describes the corresponding orientation angle of each optical element. δ_1 and δ_2 are the wavelength-dependent phase retardances of the 1st and 2nd rotating compensators. By multiplying the matrices in Eq. (7), we can obtain the following expression for the irradiance at the detector (proportional to the first element of $\mathbf{S}_{\mathrm{out}}$)

$$
\begin{aligned}
I(t) &= I_{00}M_{11}\left\{a_0 + \sum_{n=1}^{16}\left[a_{2n}\cos(2n\omega t - \phi_{2n}) + b_{2n}\sin(2n\omega t - \phi_{2n})\right]\right\} \\
&= I_0\left\{1 + \sum_{n=1}^{16}\left[\alpha_{2n}\cos(2n\omega t - \phi_{2n}) + \beta_{2n}\sin(2n\omega t - \phi_{2n})\right]\right\}
\end{aligned}
\qquad (8)
$$

where I_{00} is the spectral response function and ϕ_{2n} is the angular phase shift. $I_0 = I_{00}M_{11}a_0$, $\alpha_{2n} = a_{2n}/a_0$, $\beta_{2n} = b_{2n}/a_0$ are the d.c. and d.c.-normalized a.c. harmonic coefficients, respectively. The sample Mueller matrix elements M_{ij} (i, j = 1, 2, 3, 4) are linear combinations of α_{2n} and β_{2n}. By performing Fourier analysis [26], the sample Mueller matrix elements can be extracted from these harmonic coefficients.
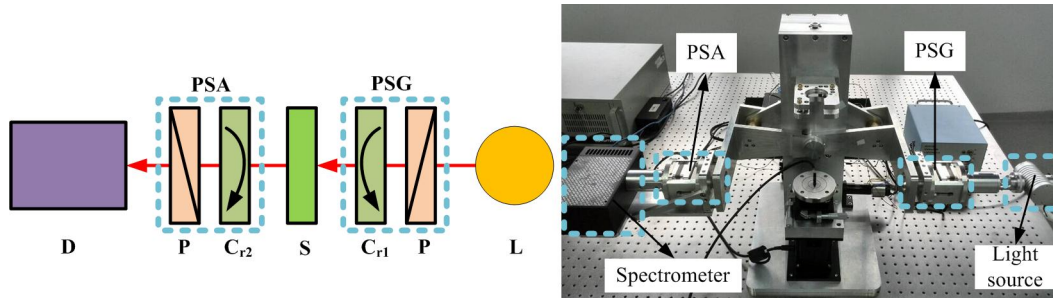
Fig. 4. Left: Schematic of the DRC-MME with L, P, C_{r1}, S, C_{r2}, A, and D denoting the light source, the polarizer, the first rotating-compensator, the sample, the second rotating-compensator, the analyzer, and the detector, respectively. Right: the home-made DRC-MME prototype.

The retardances of the rotating compensators, original axis azimuths of the polarized elements as well as imperfections in optical components must be determined before performing measurements. These systematic parameters can be obtained by performing a regression calibration procedure [27] or solving functions of the Fourier coefficients [7, 25]. In the calibration, the systematic parameters especially the retardances are wavelength-dependent and can be described by dispersion expressions or wavelength-by-wavelength data sets. But for a certain wavelength, the retardance of the compensator is usually treated as a constant during the rotation by assuming the light entering the compensator at normal incidence.

Based on the above measurement and calibration principles, we constructed a DRC-MME prototype, as depicted in Fig. 4. The rotating compensators are commercial MgF_2 biplates as described in Subsection 2.1. Although the available spectral range can be from 200 to 1000 nm, we carry out the experiments in the range from 250 to 450 nm in which the ratardance of the biplate leads to relative well-conditioned instrument configuration [18]. In this paper, we performed the experiments in the straight-through measurement mode as shown in Fig. 4.

3.2 Measurement errors induced by axis tilt in DRC-MME

In the DRC-MME, the biplates rotate with the motors and continuously modulate the polarized light. The azimuths of the 1st and 2nd rotating biplates can be described as

$$\theta_1(t) = C_1 = 5\omega t + C_{01}, \qquad (9a)$$

$$\theta_2(t) = C_2 = 3\omega t + C_{02}, \qquad (9a)$$

where C_{01} and C_{02} denote the original axis azimuths of the 1st and 2nd rotating biplates, respectively.

In practice, the biplate invariably has tilt error ε between its rotation axis and the beam due to improper installation or improper commissioning of the optical path. As described in Sec. 2, the axis tilt error will further result in periodic vibration in the retardance. The vibration in the retardance is given by

$$\Delta\delta_i(t) = \delta[\varepsilon_i, \theta_i(t)] - \delta_0[0, \theta_i(t)], \tag{10}$$

where the subscript $i = 1, 2$ denotes the i-th biplate compensator, $\delta[\varepsilon_i, \theta_i(t)]$ and $\delta_0[0, \theta_i(t)]$ can be obtained by Eq. (6), ε_i and $\theta_i(t)$ refer to the axis tilt error and azimuth of the i-th biplate.

The varied component in the retardance leads to another kind of modulation similar to a photoelastic modulator [28] with much lower frequency. In this case, the polarized light is simultaneously modulated by the azimuth and the retardance of the biplate. The azimuth-modulation introduces only even harmonic coefficients, while the retardance-modulation introduces both odd and even harmonic coefficients. It is hardly to deal with both of them in the data reduction of a MME. The common practice is to treat the retardance-modulation as spurious artifact since the azimuth-modulation is absolutely dominant in a DRC-MME. Unfortunately, this artifact is difficult even impossible to be calibrated and corrected in an azimuth-modulation DRC-MME. Therefore, measurement errors occur when such kind of axis tilt error exists.
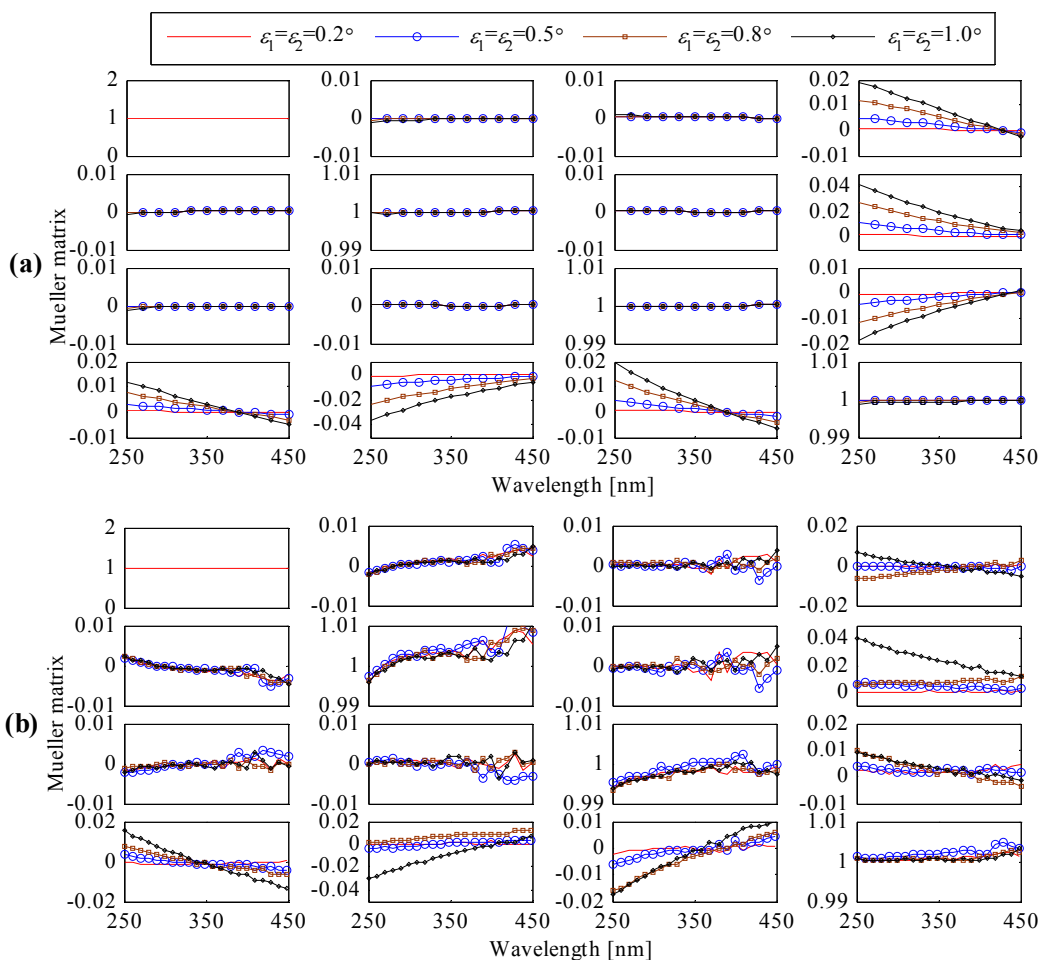
Fig. 5. Measurement errors in the normalized Mueller matrix of the air under different axis tilt errors in the biplate compensators: (a) simulated results; (b) experimental results.

Figure 5 presents the simulated and experimental results in the straight-through mode under different axis tilt errors. From Fig. 5, it can be observed that the axis tilt errors mainly affect the last row and the last column of the Mueller matrix, which means the axis tilt errors mainly have influences on the cross-talk from linear polarization to circular polarization and vice versa. The measurement errors in the Mueller matrix show positive correlations with the axis tilt

errors. In addition, these errors show strong wavelength-dependent property probably because of the wavelength-dependent configuration conditions resulted from the dispersive retardance as shown in Fig. 8. For an axis tilt error of 1°, the measurement errors in the normalized Mueller matrix of the air can be up to 0.04. If an accuracy better than 0.005 is needed for the Mueller matrix measurement, the axis tilt errors should be controlled below 0.2°. The measurement errors in the Mueller matrix of the experimental results agree to those of the simulated results, and the differences may be because of the noises and the instrument configuration errors in experiments.

To further study the measurement errors induced by the axis tilt errors, we define the distance between the measured Mueller matrix **M** and the ideal Mueller matrix $\mathbf{M}_0$ as

$$\sigma(\mathbf{M}) = \sqrt{\frac{\sum_{i=1,j=1}^{4,4} \left[\mathbf{M}(i,j) - \mathbf{M}_0(i,j)\right]^2}{16}}. \tag{11}$$
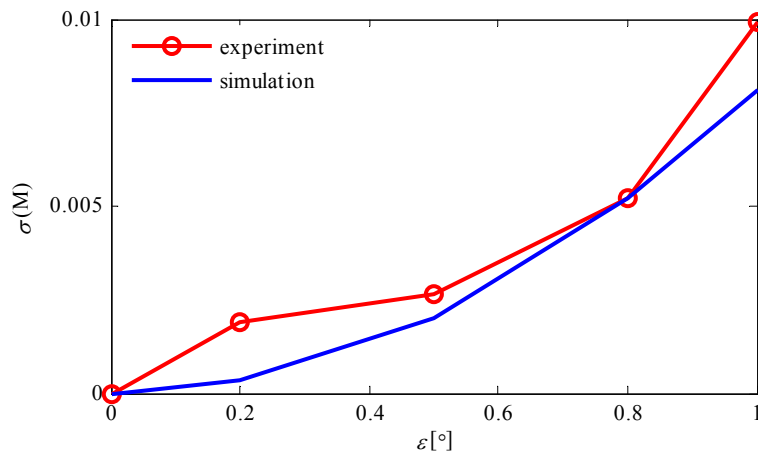
Fig. 6. Mueller distance of the DRC-MME in straight-through measurement mode versus axis tilt errors in the biplate compensators at the wavelength of 250nm.
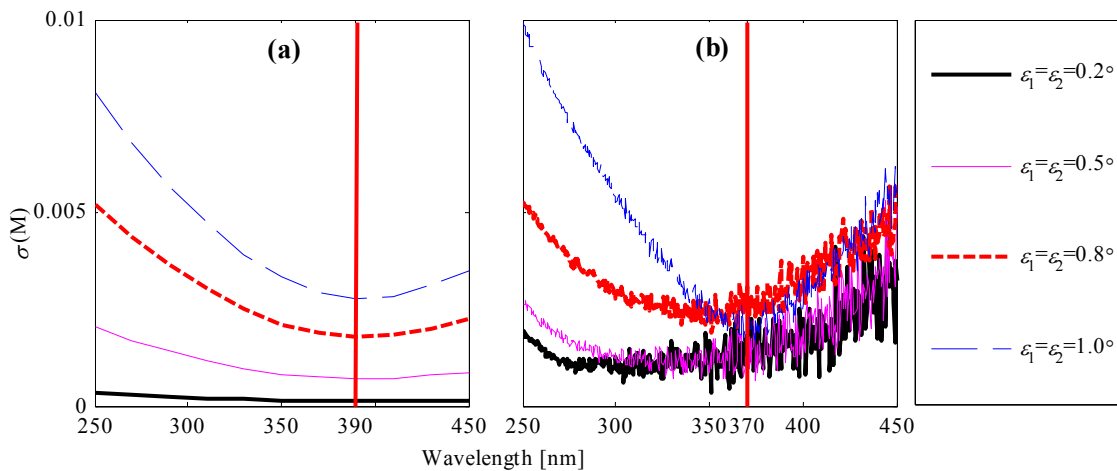
Fig. 7. Mueller distance spectra of the DRC-MME in straight-through measurement mode under different axis tilt errors in the biplate compensators: (a) simulated results; (b) experimental results.

The Mueller distances of the simulated and the experiment results show high agreement as presented in Fig. 6 and Fig. 7. It can be seen from Fig. 6 that the measurement errors in Mueller matrix increase acceleratively with the axis tilt errors in biplates. Thus, if we want to obtain an accurate Mueller matrix of the sample, the axis tilt errors should be controlled as low as 0.2°. From Fig. 7, we can obesrve that the lowest points of the simulated and the experiment results are at 390nm and 370nm, respectively. The retardances of MgF$_2$ biplates at these lowest points are about 80° for both simulations and

experiments as shown in Fig. 8. Therefore, the optimal retardance for reducing the measurement errors induced by the axis tilt errors should be 80° instead of 127° which provide the best precision [18]. However, measurements under this condition contain much more noise as shown in Fig. 7(b). In practice, we need compromise the effects of the axis tilt errors and the random noises to choose the biplates for a DRC-MME.
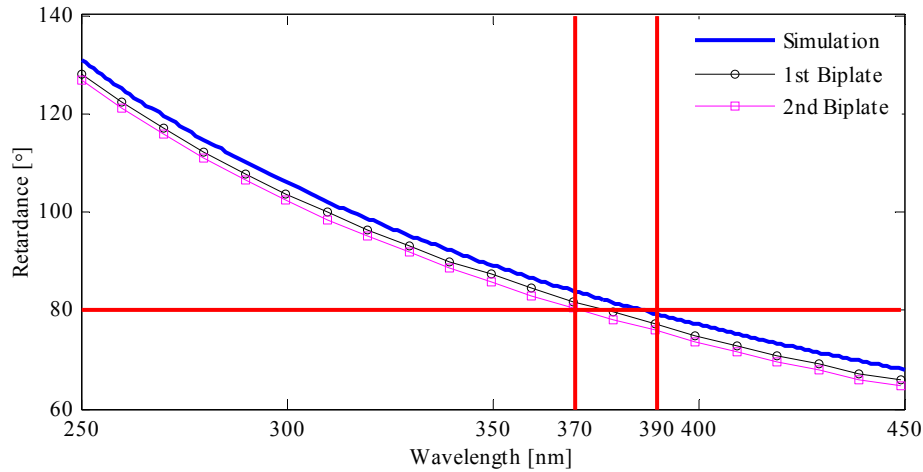
Fig. 8. Retardance spectra of the MgF$_2$ biplates for the simulations and experiments.

4. CONCLUSIONS

In this paper, a simple but valid formula for retardance calculation of biplates under arbitrary tilt angle and azimuthal angle is derived and verified. Based on the formula, different axis tilt errors in the rotating biplates and their effects on the measurement of the DRC-MME are analyzed and discussed. In a rotating-compensator system, the axis tilt error between the rotation axis and the light beam leads to a continuous vibration in the biplate retardance and is usually difficult to be calibrated and corrected. A home-made DRC-MME prototype using MgF$_2$ biplates as the rotating compensators is constructed to perform the experiments. Results demonstrate that the axis tilt errors mainly affect the cross-talk from linear polarization to circular polarization and vice versa. The measurement errors in Mueller matrix increase acceleratively with the axis tilt errors in biplates, and the measurement errors in the normalized Mueller matrix of the air can be up to 0.04 for an axis tilt error of 1°. The optimal retardance for reducing the influences of the axis tilt errors should be 80° instead of 127° which provide the best precision. This work also provides some guidences in DRC-MME design: (1) the axis tilt errors in biplates should be controlled below 0.2° if an accuracy better than 0.005 in the Mueller matrix is needed; (2) in practical selection of biplates for a DRC-MME, the effects of the axis tilt errors and the random noises should be compromised.

ACKNOWLEDGEMENTS

REFERENCES

[1] S. Y. Liu, X. G. Chen, and C. W. Zhang, "Development of a broadband Mueller matrix ellipsometer as a powerful tool for nanostructure metrology," Thin Solid Films, DOI: 10.1016/j.tsf.2015.02.006 (2015).
[2] X. G. Chen, S. Y. Liu, and C. W. Zhang, "Depolarization effects from nanoimprinted grating structures as measured by Mueller matrix polarimetry," Appl. Phys. Lett. **103**(15), 151605 (2013).

[3] X. G. Chen, S. Y. Liu, C. W. Zhang, H. Jiang, Z. C. Ma, T. Y. Sun, and Xu, Z. M., "Accurate characterization of nanoimprinted resist patterns using Mueller matrix ellipsometry," Opt. Express **22**(12), 15165-15177 (2014).

[4] X. G. Chen, C. W. Zhang, S. Y. Liu, H. Jiang, Z. C. Ma, and Z. M. Xu, "Mueller matrix ellipsometric detection of profile asymmetry in nanoimprinted grating structures," J. Appl. Phys. **116**(19), 194305 (2014).

[5] J. Lee, J. Koh, and R. W. Collins, "Multichannel Mueller matrix ellipsometer for real-time spectroscopy of anisotropic surfaces and films," Opt. Lett. **25**(21), 1573-1575 (2000).

[6] D. E. Aspnes, "Spectroscopic ellipsometry — Past, present, and future," Thin Solid Films, **571**, 334-344 (2014).

[7] J. Lee, P. I. Rovira, I. An, and R. W. Collins, "Alignment and calibration of the MgF2 biplate compensator for applications in rotating-compensator multichannel ellipsometry," J. Opt. Soc. Am. A **18**(8), 1980-1985 (2001).

[8] D. E. Aspnes, "Alignment of an optically active biplate compensator," Appl. Opt. **10**(11), 2545-2546 (1971).

[9] P. D. Hale and G. W. Day, "Stability of birefringent linear retarders (waveplates)," Appl. Opt. **27**(24), 5146-5153 (1988).

[10] E. A. West and M. H. Smith, "Polarization errors associated with birefringent waveplates," Opt. Eng. **34**(6), 1574-1580 (1995).

[11] B. Boulbry, B. Bousquet, B. L. Jeune, Y. Guern, and J. Lotrian, "Polarization errors associated with zero-order achromatic quarter-wave plates in the whole visible spectral range," Opt. Express **9**(5), 225-235 (2001).

[12] K. Ebert and D. E. Aspnes, "Biplate artifacts in rotating-compensator ellipsometers," Thin Solid Films **455-456**, 779-783 (2004).

[13] P. Marsik and J. Humlicek, "Multi-plate misalignment artifacts in rotating-compensator ellipsometry: Analysis and data treatment," Phys. Status Solidi C **5**(5), 1064–1067 (2008).

[14] H. Dong, M. Tang, and Y. D. Gong, "Measurement errors induced by deformation of optical axes of achromatic waveplate retarders in RRFP Stokes polarimeters," Opt. Express **20**(24), 26649–26666 (2012).

[15] H. Dong, P. Shum, Y. D. Gong, and Q. Z. Sun, "Measurement errors induced by retardance deviation in a rotatable retarder fixed polarizer Stokes polarimeter," Opt. Eng. **51**(3), 033001 (2012).

[16] H. Dai and C. X. Yan, "Measurement errors resulted from misalignment errors of the retarder in a rotating-retarder complete Stokes polarimeter," Opt. Express **22**(9), 11869-11883 (2014).

[17] H. G. Gu, S. Y. Liu, X. G. Chen, and C. W. Zhang, "Calibration of misalignment errors in composite waveplates using Mueller matrix ellipsometry," Appl. Opt. **54**(4), 684-693 (2015).

[18] M. H. Smith, "Optimization of a dual-rotating-retarder Mueller matrix polarimeter," Appl. Opt. **41**(13), 2488-2493 (2002).

[19] W. Q. Zhang, "General ray-tracing formulas for crystal," Appl. Opt. **31**(34), 7328-7331 (1992).

[20] F. E. Veiras, L. I. Perez, and M. T. Garea, "Phase shift formulas in uniaxial media: an application to waveplates," Appl. Opt. **49**(15), 2769-2777 (2010).

[21] M. Avendano-Alejo and M. Rosete-Aguilar, "Optical path difference in a plane-parallel uniaxial plate," J. Opt. Soc. Am. A **23**(4), 926-932 (2006).

[22] M. Bass and V. N. Mahajan, [Handbook of Optics (3rd Edition), Volume I: Geometrical and Physical Optics, Polarized Light, Components and Instruments], McGraw-Hill, 13.2-13.5 (2010).

[23] H. Nomura and Y. Furutono, "Polarimetry of illumination for 193-nm lithography used for the manufacture of high-end LSIs," Proc. SPIE **6834**, 683408 (2007).

[24] X. G. Chen, S. Y. Liu, H. G. Gu, and C. W. Zhang, "Formulation of error propagation and estimation in grating reconstruction by a dual-rotating compensator Mueller matrix polarimeter," Thin Solid Films **571**, 653-659 (2014).

[25] R. W. Collins and J. Koh, "Dual rotating-compensator multichannel ellipsometer: instrument design for real-time Mueller matrix spectroscopy of surfaces and films," J. Opt. Soc. Am. A **16**(8), 1997-2006 (1999).

[26] R. M. A. Azzam, "Photopolarimetric measurement of the Mueller matrix by Fourier analysis of a single detected signal," Opt. Lett. **2**(6), 148-150 (1978).

[27] B. Johs, "Regression calibration method for rotating element ellipsometers," Thin Solid Films **234**, 395-398 (1993).

[28] G. E. Jellison, Jr., and F. A. Modine, "Two-modulator generalized ellipsometry: theory," Appl. Opt. **36**(31), 8190-8198 (1997).